

## Free vibration analysis of a rotating non-uniform functionally graded beam

Farzad Ebrahimi\* and Samaneh Dashti

*Mechanical Engineering department, faculty of engineering,  
Imam Khomeini International University, P.O.B. 16818-34149, Qazvin, Iran*

*(Received August 26, 2014, Revised March 25, 2015, Accepted May 12, 2015)*

**Abstract.** In this paper, free vibration characteristics of a rotating double tapered functionally graded beam is investigated. Material properties of the beam vary continuously through thickness direction according to the power-law distribution of the volume fraction of the constituents. The governing differential equations of motion are derived using the Hamilton's principle and solved utilizing an efficient and semi-analytical technique called the Differential Transform Method (DTM). Several important aspects such as taper ratios, rotational speed, hub radius, as well as the material volume fraction index which have impacts on natural frequencies of such beams are investigated and discussed in detail. Numerical results are tabulated in several tables and figures. In order to demonstrate the validity and accuracy of the current analysis, some of present results are compared with previous results in the literature and an excellent agreement is observed. It is showed that the natural frequencies of an FG rotating double tapered beam can be obtained with high accuracy by using DTM. It is also observed that nondimensional rotational speed, height taper ratio, power-law exponent significantly affect the natural frequencies of the FG double tapered beam while the effects of hub radius and breadth taper ratio are negligible.

**Keywords:** free vibration analysis; non-uniform rotating beam; functionally graded material; differential transform method

---

### 1. Introduction

Differential transform method (DTM) was first introduced by Zhou (1986) in solving linear and non-linear initial value problems in electrical circuit analysis with simplicity and good precision. This method is a semi-analytical-numerical technique based on Taylor series expansion developed for various types of differential equations. DTM make possible to obtain highly convergent and accurate results and exact solutions for differential or integro-differential equations. By using this method, the governing differential equations can be reduced to recurrence relations and the boundary conditions may be transformed into a set of algebraic equations. DTM do not pose any restrictions on both the type of material gradation and the variation of the cross section profile; hence it could cover most of the engineering problems dealing with the mechanical behavior of non-uniform and non-homogenous structures.

---

\*Corresponding author, Ph.D., E-mail: febrahimi@eng.ikiu.ac.ir

Furthermore, functionally graded materials (FGMs) are the new class of composite materials which introduced by Japanese scientists in the mid-1980s as ultra-high temperature-resistant materials for aerospace applications (Tounsi *et al.* 2013, Zidi *et al.* 2014, Bouderba *et al.* 2013, Ebrahimi 2013). This kind of material is achieved by controlling the volume fractions, microstructure, porosity, etc. of the material constituents during manufacturing, resulting in spatial gradient of macroscopic material properties of mechanical strength and thermal conductivity. As a result, in comparison with traditional composites, FGMs possess various advantages, e.g., ensuring smooth transition of stress distributions, minimization or elimination of stress concentration, and increased bonding strength along the interface of two dissimilar materials. Therefore, FGMs have received wide applications in modern industries including aerospace, mechanical, electronics, optics, chemical, biomedical, nuclear, and civil engineering to name a few during the past two decades. (Ebrahimi *et al.* 2009a, b). Motivated by these engineering applications, FGMs have received considerable attention in recent researches, specially were mainly focused on their static, dynamic and vibration characteristics (Houari *et al.* 2013, Saidi *et al.* 2013, Bourada *et al.* 2012, Bouiadjra *et al.* 2013).

In addition, the non-homogeneous beams with varying material properties are widely used in civil, mechanical and aeronautical engineering, due to the fact that they can improve distribution of strength and weight, and guarantee the structural integrity. For example, functionally graded (FG) beams made of ceramic and metal are capable of both suffering from high-temperature environment because of better thermal resistance of the ceramic phase and exhibiting stronger mechanical performance of metal phase to guarantee the structural integrity of FGMs. However, in comparison with FGM shells and plates (Meziane *et al.* 2014, Draiche *et al.* 2014, Belabed *et al.* 2014, Hebali *et al.* 2014, Bessaim *et al.* 2013); there are fewer researches on FGM beams in literature. Among those, Benatta *et al.* (2008) investigated the static behaviour of FG short beams including warping and shear deformation effects. Furthermore, an analytical model for free vibration of temperature-dependent FG beams with general boundary conditions was presented by Mahi *et al.* (2010). Besides, Sina *et al.* (2009) proposed a new beam theory which is a little different from first-order shear deformation beam theory in order to analyze the free vibration of non-rotating FG beams based on an analytical method. Similarly, a new first shear deformation beam theory based on neutral surface position for functionally graded beams was developed by Bouremana *et al.* (2013). Meanwhile, Şimşek (2010) has investigated free vibration response of non-rotating FG beam for different higher order beam theories. Recently Larbi *et al.* (2013) presented an efficient shear deformation beam theory based on neutral surface position for bending and free vibration of FG beams.

Moreover, the rotating beams are extensively used in the modeling of engineering applications such as turbo-machine and turbine blades, airplane propellers and robot manipulators. For instance, the dynamic modeling and analysis of rotating blades made of FGMs has become a topic of considerable research over the last decade. The dynamic behavior of a rotating thin-walled FG blade in high temperature supersonic gas flow was investigated by Fazelzadeh and Hosseini (2007) and Fazelzadeh *et al.* (2007) by using the differential quadrature method and Galerkin method. Meanwhile, Piovan and Sampaio (2009) have developed a new finite element model to study the vibrational behavior of FG rotating beams. Likewise, a finite element approach to study the vibrational behavior of sandwich and ordinary rotating FG beams was proposed by Mohanty *et al.* (2013). Furthermore Attarnejad and Shahba (2011) examined the free vibration of non-prismatic beams by introducing the basic displacement functions for deriving shape functions in the finite element method. This methodology also has been used to study the rotating, axially FG tapered

beams by Zarrinzadeh *et al.* (2012). Furthermore, Shahba and Rajasekaran (2012) have investigated the free vibration of centrifugally stiffened tapered FG beams. Finally, on the basis of differential quadrature method, Rajasekaran (2013) has represented the free vibration analysis of a rotating, axially FG tapered beam. Most recently Li *et al.* (2014) has introduced the free vibration analysis of a rotating hub–FGM beam system with the dynamic stiffening effect based on a rigid–flexible coupled dynamics theory. However, in these formulations the FG beam has been assumed to be uniform and/or the material properties of FG beam were assumed to vary along the length of the beam while it is commonly not applicable in real structures.

Moreover, due to the fact that a non-uniform beam can be partitioned into multi homogeneous uniform sub-beams, a numerical method for determining vibrational behavior of a non-uniform beam developed by Singh *et al.* (2006). Also the functional perturbation method has been exploited by Nachum and Altus (2007) to calculate the natural frequencies and mode shapes of rods and beams with stochastic non-homogeneous properties. Furthermore, a new approach for calculating free vibration of non-uniform FG beams with varying longitudinally physical properties was proposed by Huang and Li (2010). Likewise, Alshorbagy *et al.* (2011) investigated the dynamic behaviors of the FG beams, with power law varying properties through the thickness or longitudinal directions by employing numerical finite element method.

As stated before, the differential transforms method reduces the computational difficulties of the other methods since all the calculations can be made with a simple iterative process and obtains exact results with a rapid convergence. Hence this method has recently attracted the attention of scientists in various fields of engineering. Among those, Özdemir and Kaya (2006) employed DTM to study bending vibration of a rotating tapered cantilever Bernoulli–Euler beam. Balkaya and Kaya (2009) represented the vibrating behavior of Euler–Bernoulli and Timoshenko beams resting on an elastic foundation by DTM. They recognized that the solution procedure can be easily applied to governing equation of beam vibration. Moreover Attarnejad *et al.* (2010) determined the natural frequency of a Timoshenko beam resting on two-parameter elastic foundation employing DTM.

As seen in the literature above, the DTM has been used for solving a vast range of problems in different fields of engineering; however, to the best knowledge of the authors, no research effort has been devoted so far to find the solution of vibrational behavior of a double tapered FG rotating beam by employing DTM. Motivated by these considerations, in the present study, utilizing the DTM, the free vibration of a rotating double tapered beam composed of functionally graded material is investigated in conjunction with Euler–Bernoulli beam theory. The governing differential equations of motion are derived using the Hamilton's principle and the differential transform method is utilized to obtain a semi-analytical solution to the free transverse vibration problem. Some illustrative numerical examples are presented in order to investigate the influences of FG material volume fraction index, rotational speed, hub radius, and the taper ratios on natural frequencies of tapered rotating FG beam in detail. To verify the present analysis, the results of this study are compared with the available results from the existing literature and an excellent agreement is observed.

## 2. Theory and formulation

### 2.1 Power-law functionally graded material (P-FGM) beam

One of the most favorable models for FGMs is the power-law model, in which material

properties of FGMs are assumed to vary according to a power law about spatial coordinates. As shown in Fig. 1 a non-uniform flexible beam made of FGMs with length  $L$  is attached to periphery of a rigid hub of radius  $R$  and the hub rotates about vertical  $z$  axis in a fixed coordinate system at a constant angular speed  $\Omega$ . The beam tapers linearly from a height  $h_0$  at the root to  $h$  at the free end in the  $xz$  plane and from a breadth  $b_0$  to  $b$  in the  $xy$  plane. The height taper ratio,  $\beta$  and the breadth taper ratio,  $\alpha$ , whose descriptions are going to be given in the following sections must be  $\beta < 1$  and  $\alpha < 1$  because otherwise the beam tapers to zero between its ends. A Cartesian coordinate system  $O(x, y, z)$  is defined on the central axis of the beam where the  $x$  axis is taken along the central axis, the  $y$ -axis in the width direction and the  $z$ -axis in the depth direction. The FG beam is assumed to be composed of ceramic and metal and effective material properties ( $P_f$ ) of the FG beam such as Young's modulus  $E_f$ , shear modulus  $G_f$  and mass density  $\rho_f$  are assumed to vary continuously in the thickness direction ( $z$ -axis direction) according to a power function of the volume fractions of the constituents while the Poisson's ratio is assumed to be constant (Li 2008). According to the rule of mixture, the effective material properties,  $P$ , can be expressed as (Şimşek 2010)

$$P_f = P_c V_c + P_m V_m \quad (1)$$

Where  $P_m$ ,  $P_c$ ,  $V_m$  and  $V_c$  are the material properties and the volume fractions of the metal and the ceramic constituents related by

$$V_c + V_m = 1 \quad (2)$$

The volume fraction of the metal constituent of the beam is assumed to be given by

$$V_c = \left( \frac{z}{h} + \frac{1}{2} \right)^n \quad (3)$$

Here  $n$  is the non-negative variable parameter (power-law exponent) which determines the material distribution through the thickness of the beam. Therefore, from Eqs. (1)-(3), the effective material properties of the FG beam can be expressed as follows

$$P_f(z) = (P_c - P_m) \left( \frac{z}{h} + \frac{1}{2} \right)^n + P_m \quad (4)$$

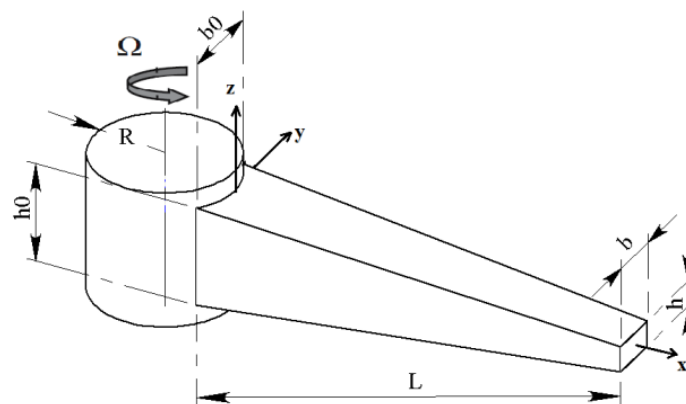


Fig. 1 Geometry of the of a rotating hub-double tapered FG beam system

According to this distribution, bottom surface ( $z = -h/2$ ) of FG beam is pure metal, whereas the top surface ( $z = h/2$ ) is pure ceramics.

## 2.2 Formulation of rotating double tapered FGM beam

In a Cartesian coordinate system,  $x$  is the distance of the point from the hub edge parallel to beam length,  $u_0$  is the axial displacement due to the centrifugal force;  $z$  is the vertical distance of the point from the middle plane,  $w$  is the transverse displacement of any point on the neutral axis. Displacement field components are considered based on Euler–Bernoulli beam theory. Considering Kirchhoff–Love hypothesis, the strain energy relations for the rotating FG beam are calculated as follows (Hodges and Rutkowski 1981)

$$U = \frac{1}{2} \left( \int_0^L C(x) \dot{W}^2 dx + \int_0^L T(x) \dot{W}^2 dx \right) \quad (5)$$

Here  $T(x)$  denotes the centrifugal force that varies along the spanwise direction of the beam is defined as

$$T(x) = \int_x^L D(x) \Omega^2 (R + x) dx \quad (6)$$

Also the kinetic energy expression is given as

$$T = \int_0^L \frac{1}{2} D(x) \dot{W}^2 dx \quad (7)$$

In which the bending rigidity  $C(x)$  of the beam cross section and the normal inertia term of the beam  $D(x)$  are respectively defined as

$$C(x) = \int_A E(z) z(x)^2 dA(x) \quad (8a)$$

$$D(x) = \int_A \rho(z) dA(x) \quad (8b)$$

Where  $\rho$  and  $E$  are the mass density and modulus of elasticity of the FG beam respectively. It is worth mentioning that  $A$  is a function of  $x$  since cross-sectional profile changes along the longitudinal axis. Eq. (8a) can be written as

$$C(x) = \int_{-\frac{h}{2}}^{\frac{h}{2}} E(z) z^2 b(x) dz = b(x) h(x)^3 \tilde{E} \quad (9a)$$

where

$$\tilde{E} = (E_c - E_m) \left( \frac{1}{n+3} - \frac{1}{n+2} + \frac{1}{4(n+1)} \right) + \frac{E_m}{12} \quad (9b)$$

Now defining  $C_0 = b_0 h_0^3 \tilde{E}$ , the bending rigidity of the beam cross section may be obtained

as

$$C(x) = C_0 \left(1 - \alpha \frac{x}{L}\right) \left(1 - \beta \frac{x}{L}\right)^3 \quad (9c)$$

Similarly Eq. (8b) can be written as

$$D(x) = \int_{-h/2}^{h/2} \rho(z) b(x) dz = b(x)h(x)\tilde{\rho} = A(x)\tilde{\rho} \quad (10a)$$

in which

$$\tilde{\rho} = \frac{\rho_c - \rho_m}{n + 1} + \rho_m \quad (10b)$$

Now defining  $D_0 = A_0 \tilde{\rho}$ , the normal inertia term of the beam may be obtained as

$$D(x) = D_0 \left(1 - \alpha \frac{x}{L}\right) \left(1 - \beta \frac{x}{L}\right) \quad (10c)$$

Substituting Eq. (10c) into Eq. (6), the centrifugal force is obtained as follows

$$T(x) = D_0 \Omega^2 \int_x^L \left(1 - \alpha \frac{x}{L}\right) \left(1 - \beta \frac{x}{L}\right) (R + x) dx \quad (11)$$

Hamilton's principle is used herein to derive the equations of motion. The principle can be stated in analytical form as

$$\delta \int_{t_1}^{t_2} (T - U) dt = 0 \quad (12a)$$

Here,  $t_1$  and  $t_2$  are the initial and end time, respectively;  $\delta U$ ,  $\delta T$  are the virtual variation of the strain and kinetic energy respectively. According to Hamilton's principle, the equations of motion can be obtained as

$$D(x) \frac{\partial^2 w}{\partial t^2} + \frac{\partial^2}{\partial x^2} \left( C(x) \frac{\partial^2 w}{\partial x^2} \right) - \frac{\partial}{\partial x} \left( T(x) \frac{\partial w}{\partial x} \right) = 0 \quad (12b)$$

Further, the two ends of the cantilever beam ( $x = 0$  and  $x = L$ ) are subjected to the following boundary conditions

$$\text{at } x = 0: \quad x = 0, \quad w = \frac{\partial w}{\partial x} = 0 \quad (13a)$$

$$\text{at } x = L: \quad \frac{\partial^2 w}{\partial x^2} = \frac{\partial^3 w}{\partial x^3} = 0 \quad (13b)$$

Assuming simple harmonic oscillation,  $w$  can be written as

$$w(x, t) = \bar{w}(x)e^{i\omega t} \quad (14)$$

Substituting Eq. (14) into Eq. (12b), the governing equation is obtained as follows

$$-\omega^2 D(x) \bar{w} + \frac{d^2}{dx^2} \left( C(x) \frac{d^2 \bar{w}}{dx^2} \right) - \frac{d}{dx} \left( T(x) \frac{d\bar{w}}{dx} \right) = 0 \quad (15)$$

### 2.3 Tapered beam formulation and dimensionless parameters

The general equations for the cross-sectional area,  $A(x)$ , the height  $h(x)$ , the breadth  $b(x)$ , the second moment of area,  $I_y(x)$  of a beam that tapers in two planes and the increments along  $y$  and  $z$  axis,  $dy(x)$  and,  $dz(x)$ , are given by

$$b(x) = b_0 \left(1 - \alpha \frac{x}{L}\right)^m \quad (16a)$$

$$h(x) = h_0 \left(1 - \beta \frac{x}{L}\right)^s \quad (16b)$$

$$A(x) = A_0 \left(1 - \alpha \frac{x}{L}\right)^m \left(1 - \beta \frac{x}{L}\right)^s \quad (16c)$$

$$I_y(x) = I_{y0} \left(1 - \alpha \frac{x}{L}\right)^m \left(1 - \beta \frac{x}{L}\right)^{3s} \quad (16d)$$

$$dy(x) = dy_0 \left(1 - \alpha \frac{x}{L}\right)^m \quad (16e)$$

$$dz(x) = dz_0 \left(1 - \beta \frac{x}{L}\right)^s \quad (16f)$$

In which the breadth taper ratio,  $\alpha$  and the height taper ratio,  $\beta$  are given by

$$\alpha = 1 - \frac{b}{b_0} \quad (17a)$$

$$\beta = 1 - \frac{h}{h_0} \quad (17b)$$

Values of  $s = 1$  and  $m = 1$  are used in this study to model the beam that tapers linearly in two planes. Knowing that the subscript  $()_o$  denotes the values at the root of the beam, the following formulas can be introduced

$$A_0 = b_0 h_0 \quad (18)$$

$$I_{y0} = \frac{b_0 h_0^3}{12} \quad (19)$$

The dimensionless parameters which founded according to FGM characteristics are used to simplify the equations and to make comparisons with the studies in literature such as (Şimşek 2010) can be given as follows

$$\delta = \frac{R}{L}, \quad \xi = \frac{x}{L}, \quad \tilde{w} = \frac{\bar{W}}{L}, \quad \eta^2 = \frac{D_0 L^4 \Omega^2}{C_0}, \quad \mu^2 = \frac{D_0 L^4 \omega^2}{C_0} \quad (20)$$

Here  $\delta$  is the hub radius parameter,  $\eta$  is the rotational speed parameter,  $\mu$  is the frequency parameter,  $\xi$  is the dimensionless distance and  $\tilde{w}$  is the dimensionless flapwise deformation.

Then substituting Eqs. (16)-(20) into Eq. (11) and substituting the resulted relation into Eq. (15) the dimensionless expressions for centrifugal force and the governing equation are obtained respectively as follows

$$T(\xi) = D_0 \Omega^2 L^2 \left[ \frac{\alpha\beta}{4} + \delta - \frac{1}{2}(\alpha\delta + \beta\delta - 1) - \frac{1}{3}(\alpha + \beta - \alpha\beta\delta) - \xi\delta + \frac{\xi^2}{2}(\alpha\delta + \beta\delta - 1) + \frac{\xi^3}{3}(\alpha + \beta - \alpha\beta\delta) - \frac{\xi^4}{4}\alpha\beta \right] \quad (21)$$

$$\begin{aligned} & \frac{d^2}{d\xi^2} \left[ (1 - \alpha\xi)(1 - \beta\xi)^3 \frac{d^2 \tilde{w}}{d\xi^2} \right] - \mu^2 (1 - \alpha\xi)(1 - \beta\xi) \tilde{w} \\ & - \eta^2 \frac{d}{d\xi} \left\{ \left[ \frac{\alpha\beta}{4} (1 - \xi^4) + \delta(1 - \xi) + \frac{1}{2}(1 - \alpha\delta - \beta\delta)(1 - \xi^2) + \frac{1}{3}(-\alpha - \beta + \alpha\beta\delta)(1 - \xi^3) \right] \frac{d\tilde{w}}{d\xi} \right\} = 0 \end{aligned} \quad (22)$$

#### 2.4 Implementation of differential transform method

Generally, it is rather difficult to derive an analytical solution for Eq. (22) due to the nature of non-homogeneity. In this circumstance, the DTM is employed to translate the governing equations into a set of ordinary equations. First, the procedure of differential transform method is briefly reviewed. The differential transforms method provides an analytical solution procedure in the form of polynomials to solve ordinary and partial differential equations. In this method, differential transformation of  $k$ th derivative function  $y(x)$  and differential inverse transformation of  $Y(k)$  are respectively defined as follows (Abdel-Halim Hassan 2002)

$$Y(k) = \frac{1}{k!} \left[ \frac{d^k}{dx^k} y(x) \right]_{x=0} \quad (23a)$$

$$y(x) = \sum_0^{\infty} x^k Y(k) \quad (23b)$$

In which  $y(x)$  is the original function and  $Y(k)$  is the transformed function. Consequently from Eqs. (23a) and (23b) we obtain

$$y(x) = \sum_{k=0}^{\infty} \frac{x^k}{k!} \left[ \frac{d^k}{dx^k} y(x) \right]_{x=0} \quad (24)$$

Eq. (24) reveals that the concept of the differential transformation is derived from Taylor's series expansion. In real applications the function  $y(x)$  in Eq. (24) can be written in a finite form as

$$y(x) = \sum_{k=0}^N x^k Y(k) \quad (25)$$

In this calculations  $y(x) = \sum_{n+1}^{\infty} x^k Y(k)$  is small enough to be neglected, and  $N$  is determined by the convergence of the eigenvalues. From the definitions of DTM in Eqs. (23) and (24), the

Table 1 Some of the transformation rules of the one-dimensional DTM

Original function	Transformed function
$y(x) = \lambda\varphi(x)$	$Y(k) = \lambda\Phi(k)$
$y(x) = \varphi(x) \pm \theta(x)$	$Y(k) = \Phi(k) \pm \Theta(k)$
$y(x) = \frac{d\varphi}{dx}$	$Y(k) = (k+1)\Phi(k+1)$
$y(x) = \frac{d^2\varphi}{dx^2}$	$Y(k) = (k+1)(k+2)\Phi(k+2)$
$y(x) = \varphi(x)\theta(x)$	$Y(k) = \sum_{l=0}^k \Phi(l)\Theta(k-l)$
$y(x) = x^m$	$Y(k) = \delta(k-m) = \begin{cases} 1 & k = m \\ 0 & k \neq m \end{cases}$

fundamental theorems of differential transforms method can be performed that are listed in Table 1 while Table 2 presents the differential transformation of conventional boundary conditions

Applying the DTM rule on the equation of motion the following equation is obtained

$$\begin{aligned}
& \left[ \frac{\alpha\beta}{4}(k+1)(k-2)\eta^2 - \alpha\beta\mu^2 \right] W[k-2] \\
& + \left[ \frac{1}{3}(-\alpha - \beta + \alpha\beta\delta)\eta^2(k-1)(k+1) + (\alpha + \beta)\mu^2 \right] W[k-1] \\
& + \left[ \alpha\beta^3(k-1)k(k+1)(k+2) + \frac{1}{2}(-\alpha\delta - \beta\delta + 1)k(k+1)\eta^2 - \mu^2 \right] W[k] \\
& + [-\beta^2(3\alpha + \beta)(k+2)(k+1)^2k + (k+1)^2\delta\eta^2] W[k+1] \\
& + \{3\beta(\alpha + \beta)(k+1)^2(k+2)^2 + \eta^2(k+1)(k+2) \\
& \quad \frac{1}{2}(-1 + \alpha\delta + \beta\delta) + \frac{1}{3}(\alpha + \beta - \beta\alpha\delta) - \left(\frac{1}{4}\alpha\beta + \delta\right)\} \\
& \quad W[k+2] - [(k+1)(k+2)^2(k+3)(\alpha + 3\beta)]W[k+3] \\
& + (k+1)(k+2)(k+3)(k+4)W[k+4] = 0
\end{aligned} \tag{26}$$

Additionally, the differential transform method is applied to boundary conditions by using the theorems introduced in Table 2 and the following transformed boundary conditions are obtained

$$\xi = 0 : \quad W[0] = W[1] = 0 \tag{27}$$

$$\xi = 1 : \quad \sum_{k=2}^{\infty} k(k-1)W[k] = 0, \quad \sum_{k=3}^{\infty} k(k-1)(k-2)W[k] = 0 \tag{28}$$

Here,  $W(k)$  is the differential transforms of  $w(\xi)$ . The values of  $W[2]$  and  $W[3]$  are assumed to be  $c_1$  and  $c_2$  respectively where  $c_1$  and  $c_2$  are constants. Using Eq. (26) the values of  $W(k)$  for  $k = 4, 5, 6, \dots$  can be obtained. Now substituting the obtained  $W(k)$  into Eq. (28) we arrive at following two polynomial equations

Table 2 Transformed boundary conditions (B.C.) based on DTM

X = 0		X = 1	
Original BC	Transformed BC	Original BC	Transformed BC
$f(0) = 0$	$F[0] = 0$	$f(1) = 0$	$\sum_{k=0}^{\infty} F[k] = 0$
$\frac{df}{dx}(0) = 0$	$F[1] = 0$	$\frac{df}{dx}(1) = 0$	$\sum_{k=0}^{\infty} kF[k] = 0$
$\frac{d^2f}{dx^2}(0) = 0$	$F[2] = 0$	$\frac{d^2f}{dx^2}(1) = 0$	$\sum_{k=0}^{\infty} k(k-1)F[k] = 0$
$\frac{d^3f}{dx^3}(0) = 0$	$F[3] = 0$	$\frac{d^3f}{dx^3}(1) = 0$	$\sum_{k=0}^{\infty} k(k-1)(k-2)F[k] = 0$

$$M_{j1}^{(q)} c_1 + M_{j2}^{(q)} c_2 = 0, \quad j = 1, 2 \quad (29)$$

In which  $M_{ij}$  are polynomials in terms of  $\omega$  corresponding to  $q^{\text{th}}$  term. The matrix form of Eq. (29) can be prescribed as

$$\begin{bmatrix} M_{11}^{(q)} & M_{12}^{(q)} \\ M_{21}^{(q)} & M_{22}^{(q)} \end{bmatrix} \begin{Bmatrix} c_1 \\ c_2 \end{Bmatrix} = 0 \quad (30)$$

Further, studying the existence condition of the non-trivial solutions for Eq. (30) yields the following characteristic equation

$$\begin{vmatrix} M_{11}^{(q)} & M_{12}^{(q)} \\ M_{21}^{(q)} & M_{22}^{(q)} \end{vmatrix} = 0 \quad (31)$$

Solving Eq. (31), the  $i^{\text{th}}$  estimated eigenvalue for  $q^{\text{th}}$  iteration ( $\omega = \omega_i^{(q)}$ ) may be obtained and the total number of iterations is related to the accuracy of calculations which can be determined by the following equation

$$\left| \omega_i^{(q)} - \omega_i^{(q-1)} \right| < \varepsilon \quad (32)$$

If Eq. (32) is satisfied,  $\omega_i^{(q)}$  will be the  $i^{\text{th}}$  natural frequency. In this study  $\varepsilon = 0.0001$  considered in procedure of finding eigenvalues which results in 4 digit precision in estimated eigenvalues. The procedure of finding Eigen values iterates till Eigen values converge. Further a Matlab program has been developed according to DTM rule stated above, in order to find eigenvalues. As mentioned before, DTM method implies an iterative procedure to obtain the high-order Taylor series solution of differential equations. The Taylor series method requires a long computational time for large orders, whereas one advantage of employing DTM in solving differential equations is a fast convergence rate and a small calculation error.

### 3. Convergence and correctness study of the solution method

In order to show that differential transform method is an effective and reliable tool for examining the vibration characteristics of rotating beam, an FG rotating double tapered beam composed of a ceramic–metal pair of materials is considered. The material properties of the power-law FG constituents are presented in Table 3. Relation described in Eq. (33) is performed in order to calculate the non-dimensional natural frequencies.

$$\lambda = \frac{\omega L^2}{h} \sqrt{\frac{\rho_m}{E_m}} \quad (33)$$

Table 3 Material properties of the FGM constituents (Simsek 2010)

Properties	Unit	Aluminum	Alumina (Al <sub>2</sub> O <sub>3</sub> )
$E$	GPa	70	380
$\rho$	Kg/m <sup>3</sup>	2702	3960
$\nu$	-	0.3	0.3

Table 4 Convergence study for the first four frequencies of rotating double tapered FG beam ( $n = \delta = 0, L/h = 5, \eta = 6, \alpha = \beta = 0.2$ )

$n$	$\omega_1$	$\omega_2$	$\omega_3$	$\omega_4$
19	6876.1455	-	-	-
20	6876.8027	-	-	-
21	6876.2390	-	-	-
22	6875.7530	-	-	-
23	6875.1422	-	-	-
24	6874.5998	23222.7876	55548.2142	-
25	6874.4851	23221.2867	55549.7564	-
26	6874.4681	23221.1657	55550.1146	-
27	6874.4841	23221.4762	55549.8367	-
28	6874.5119	23221.7984	55549.5248	-
29	6874.5299	23222.0059	55549.3230	-
30	6874.5388	23222.1067	55549.2171	-
31	6874.5422	23222.1430	55549.1742	103786.4525
32	6874.5429	23222.1497	55549.1624	103788.4381
33	6874.5427	23222.1467	55549.1622	103788.1917
34	6874.5424	23222.1427	55549.1646	103788.0964
35	6874.5422	23222.1340	55549.1667	103788.1207
36	6874.5420	23222.1386	55549.1679	103788.1304
37	6874.5420	23222.1381	55549.1684	103788.1318
38	6874.5420	23222.1379	55549.1686	103788.1324
39	6874.5420	23222.1379	55549.1687	103788.1327

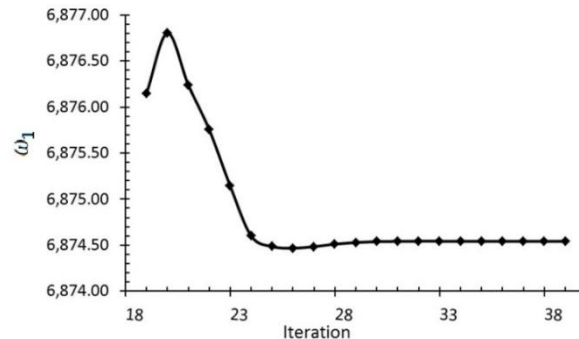


Fig. 2 Convergence study for the first frequency of rotating double tapered FG beam

Table 5 Comparison of fundamental frequencies of FG rotating uniform beams ( $\alpha = \beta = \eta = 0$ ,  $L/h = 20$ )

$n$	Present DTM	Lagrange's equations (Şimşek 2010)	Rayleigh–Ritz method (Pradhan and Chakraverty 2014)
0	1.9534	1.95248	1.9525
0.2	1.8322	1.81714	1.8171
0.5	1.7247	1.66265	1.6644
Metal	1.0214	1.01449	-

Table 4 tabulates the convergence study of DTM method for the first four frequencies of rotating double tapered FG beam. It is found that in DTM method after a certain number of iterations eigenvalues converged to a value with good precision, so the number of iterations is important in DTM method convergence. This fact is obvious in Fig. 2 which demonstrates the convergence trend for the first frequency. According to Table 4 the first natural frequency converged after 36 iterations with 4 digit precision while the other frequencies converged after 39 iterations.

After looking into the satisfactory results for the convergence of frequencies, one may compare the nondimensional frequencies of double tapered FG beam associated with different taper ratios and constituent volume fraction exponents. To demonstrate the correctness of present study the results for FG rotating beam are compared with the results of FG rotating beams available in the literature. Table 5 compares the semi-analytical results of the present study and the results obtained for the uniform FG rotating beam with various constituent volume fraction exponents presented by Şimşek (2010) which has been obtained by using Lagrange's equations and the results presented by Pradhan and Chakraverty (2014) which has been obtained by using Rayleigh–Ritz method. One may clearly notice here that the fundamental frequency parameters obtained in the present investigation are in approximately close enough to the results provided in these literatures and thus validates the proposed method of solution.

#### 4. Numerical results and discussion

After validating the approaches, in the this section some parametric studies are conducted in order to examine the influences of various FG beam parameters such as constituent volume

fractions, taper ratios, rotational speed and hub radius on the natural frequencies of the rotating double tapered FG beam. Here after, to better extract the influence of the taper ratios on the vibrational behavior of the rotating FG beams, the normalized form of the nonlinear natural frequencies as specified in Eq. (33), are presented in the numerical results. In Table 6, the variation of the first, second and third normalized frequencies of tapered FG rotating beam against the different values of both breadth taper ratio and the height taper ratio is presented. Also the effect of both breadth and the height taper ratio on the first three natural frequencies of FG rotating beam is plotted in Fig. 3. It can be seen from this figure that for the constant value of rotational speed parameter, the fundamental natural frequency of tapered FG beams increase as the breadth and the height taper ratio increase. It is concluded that the breadth taper ratio has more prominent influence on the fundamental natural frequency compared to the height taper ratio. For instance for FG beam with power-law exponent defined as  $n = 1$ , when  $\beta = 0.1$ , increasing the breadth taper ratio ( $\alpha$ ) from 0 to 0.6, leads to about 22.8% increase in the first natural frequency while when  $\alpha = 0.1$ , increasing the height taper ratio from 0 to 0.6, leads to about 9.7% increase in the first natural frequency of the tapered FG rotating beam. This effect has been studied on the higher mode frequencies as showed in Fig. 3.

Table 6 Variation of the first three non-dimensional natural frequencies of FG rotating tapered beam with various taper ratios ( $n = 1$ ,  $\delta = 0$ ,  $\eta = 2$ ,  $l/h = 20$ )

$\beta$	Mode number	$\alpha$						
		0	0.1	0.2	0.3	0.4	0.5	0.6
0	2.3717	2.2579	2.1668	2.0918	2.0289	1.9751	1.9285	$\lambda_1$
	11.4070	11.1860	11.0108	10.8660	10.7429	10.6360	10.5415	$\lambda_2$
	29.9213	29.6772	29.4920	29.3443	29.2220	29.1179	29.0274	$\lambda_3$
0.1	2.3922	2.2781	2.1868	2.1117	2.0486	1.9947	1.9480	$\lambda_1$
	11.0559	10.8423	10.6729	10.5331	10.4143	10.3111	10.2199	$\lambda_2$
	28.6351	28.3982	28.2179	28.0737	27.9540	27.8519	27.7629	$\lambda_3$
0.2	2.4159	2.3016	2.2101	2.1348	2.0715	2.0174	1.9705	$\lambda_1$
	10.6950	10.4888	10.3254	10.1907	10.0762	9.9768	9.8890	$\lambda_2$
	27.3154	27.0859	26.9108	26.7702	26.6532	26.5532	26.4658	$\lambda_3$
0.3	2.4439	2.3293	2.2375	2.1619	2.0985	2.0442	1.9971	$\lambda_1$
	10.3230	10.1243	9.9671	9.8374	9.7273	9.6318	9.5474	$\lambda_2$
	25.9565	25.7347	25.5649	25.4282	25.3141	25.2163	25.1308	$\lambda_3$
0.4	2.4775	2.3625	2.2704	2.1946	2.1308	2.0763	2.0289	$\lambda_1$
	9.9385	9.7475	9.5965	9.4721	9.3664	9.2748	9.1939	$\lambda_2$
	24.5507	24.3370	24.1728	24.0402	23.9292	23.8339	23.7503	$\lambda_3$
0.5	2.5190	2.4036	2.3111	2.2348	2.1707	2.1158	2.0681	$\lambda_1$
	9.5400	9.3568	9.2121	9.0930	8.9919	8.9043	8.8269	$\lambda_2$
	23.0878	22.8826	22.7243	22.5961	22.4885	22.3958	22.3144	$\lambda_3$
0.6	2.5717	2.4557	2.3627	2.2860	2.2214	2.1660	2.1179	$\lambda_1$
	9.1261	8.9509	8.8127	8.6989	8.6025	8.5189	8.4452	$\lambda_2$
	21.5532	21.3570	21.2050	21.0815	20.9776	20.8879	20.8090	$\lambda_3$

Fig. 4 depicts the variation of the first three frequencies versus the height taper ratio of FG rotating tapered beam. According to these figures, the second and the third normalized frequencies of tapered FG rotating beam increase when the breadth taper ratio increase and also when the height taper ratio decrease. Frequency parameters of FG rotating tapered beam affected by power-law exponent and the rotational speed parameter are studied in Table 7. Inspection of this table reveals that an increase in the value of the power-law exponent leads to a decrease in the fundamental frequencies. The highest frequency values are obtained for full ceramic beam ( $n = 0$ ) while the lowest frequency values are obtained for full metal beam ( $n \rightarrow \infty$ ). This is due to the fact that, an increase in the value of the power-law exponent results in a decrease in the value of elasticity modulus and the value of bending rigidity. In other words, the beam becomes flexible as the power law exponent increases. Therefore, as also known from mechanical vibrations, natural frequencies decrease as the stiffness of a structure decreases.

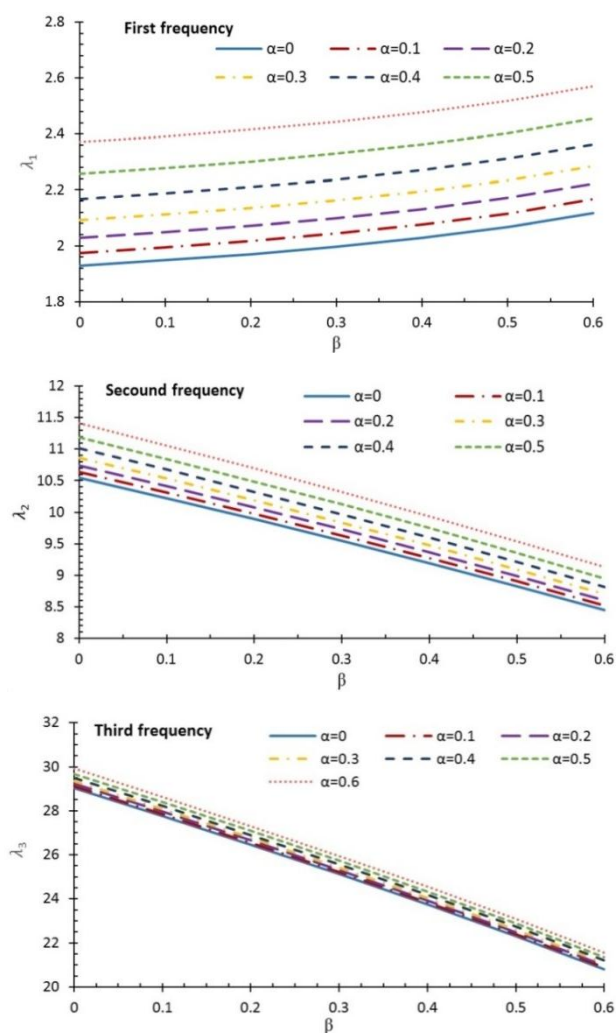


Fig. 3 The effect of taper ratios on the first three non-dimensional frequencies of FG rotating tapered beam ( $n = 1$ ,  $\delta = 0$ ,  $\eta = 2$ ,  $l/h = 20$ )

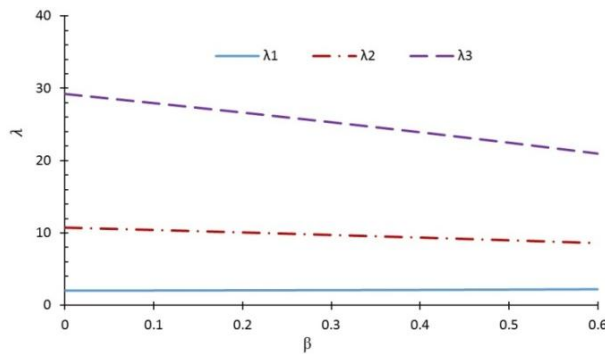


Fig. 4 The effect of height taper ratio on the first three non-dimensional frequencies of FG rotating tapered beam ( $n = 1, \alpha = 0.2, \delta = 0, \eta = 2, l/h = 20$ )

It is also interesting to note that the decrease in the frequency values due to the increase in the power-law exponent is almost the same for higher mode frequencies.

The other important parameter in vibration behavior of rotating FG tapered beam is its rotational speed parameter. Table 7 presents the variation of first four natural frequencies of FG rotating beam with various power-law exponents for different rotational speed parameters ( $\eta = 0, 2, 4, 6, 8, 10$ ). The effect of rotational speed and power-law exponent on the first natural frequency of FG rotating tapered beam has been depicted in Fig. 5. According to Fig. 5, increasing the rotational speed increases the fundamental frequency of rotating FG tapered beam and this trend is almost the same for all values of power-law exponents. This is due to the fact that, an increase in rotational speed results in an increase in the value of the centrifugal force and hence increasing the natural frequencies.

Table 7 The effect of rotational speed parameter on first four non-dimensional natural frequencies of FG rotating tapered beam with different values of the power law exponents ( $\delta = 0, L/h = 10, \alpha = \beta = 0.1$ )

$n$		$\eta$					
		0	2	4	6	8	10
0.1	$\lambda_1$	2.0410	2.3775	3.1700	4.1497	5.1999	6.2790
	$\lambda_2$	11.9729	12.2898	13.1953	14.5798	16.3194	18.3094
	$\lambda_3$	32.8841	33.1967	34.1158	35.5904	37.5490	39.9132
	$\lambda_4$	64.1128	64.4335	65.3850	66.9374	69.0450	71.6524
0.2	$\lambda_1$	1.9143	2.2299	2.9733	3.8921	4.8771	5.8893
	$\lambda_2$	11.2297	11.5270	12.3762	13.6748	15.3065	17.1729
	$\lambda_3$	30.8429	31.1361	31.9982	33.3813	35.2183	37.4358
	$\lambda_4$	60.1332	60.4340	61.3265	62.7825	64.7593	67.2049
0.5	$\lambda_1$	1.8021	2.0991	2.7989	3.6638	4.5911	5.5438
	$\lambda_2$	10.5711	10.8509	11.6503	12.8727	14.4087	16.1657
	$\lambda_3$	29.0339	29.3099	30.1214	31.4233	33.1526	35.2400
	$\lambda_4$	56.6062	56.8893	57.7295	59.1001	60.9609	63.2630

Table 7 Continued

$n$		$\eta$					
		0	2	4	6	8	10
1	$\lambda_1$	1.7124	1.9947	2.6597	3.4816	4.3627	5.2680
	$\lambda_2$	10.0452	10.3111	11.0708	12.2324	13.6919	15.3615
	$\lambda_3$	27.5896	27.8519	28.6230	29.8602	31.5034	33.4870
	$\lambda_4$	53.7903	54.0594	54.8578	56.1602	57.9285	60.1161
2	$\lambda_1$	1.6426	1.9134	2.5512	3.3396	4.1849	5.0533
	$\lambda_2$	9.6358	9.8908	10.6195	11.7338	13.1338	14.7354
	$\lambda_3$	26.4650	26.7166	27.4563	28.6431	30.2193	32.1221
	$\lambda_4$	51.5978	51.8559	52.6217	53.8710	55.5672	57.6657
5	$\lambda_1$	1.5376	1.7911	2.3882	3.1262	3.9174	4.7303
	$\lambda_2$	9.0198	9.2585	9.9407	10.9837	12.2943	13.7934
	$\lambda_3$	24.7733	25.0087	25.7012	26.8121	28.2876	30.0687
	$\lambda_4$	48.2994	48.5410	49.2579	50.4274	52.0151	53.9794
10	$\lambda_1$	1.4194	1.6533	2.2045	2.8858	3.6161	4.3665
	$\lambda_2$	8.3262	8.5466	9.1763	10.1391	11.3489	12.7327
	$\lambda_3$	22.8683	23.0857	23.7249	24.7503	26.1124	27.7565
	$\lambda_4$	44.5854	44.8084	45.4702	46.5497	48.0154	49.8286
50	$\lambda_1$	1.1762	1.3700	1.8267	2.3913	2.9965	3.6183
	$\lambda_2$	6.8994	7.0820	7.6038	8.4016	9.4041	10.5509
	$\lambda_3$	18.9496	19.1297	19.6593	20.5091	21.6377	23.0001
	$\lambda_4$	36.9452	37.1300	37.6783	38.5729	39.7874	41.2899
100	$\lambda_1$	1.1230	1.3081	1.7442	2.2832	2.8610	3.4547
	$\lambda_2$	6.5876	6.7619	7.2601	8.0219	8.9791	10.0740
	$\lambda_3$	18.0930	18.2650	18.7707	19.5821	20.6597	21.9605
	$\lambda_4$	35.2753	35.4517	35.9753	36.8294	37.9890	39.4236
Metal	$\lambda_1$	1.0672	1.2432	1.6576	2.1698	2.7190	3.2832
	$\lambda_2$	6.2606	6.4263	6.8997	7.6237	8.5333	9.5739
	$\lambda_3$	17.1949	17.3583	17.8389	18.6100	19.6341	20.8703
	$\lambda_4$	33.5241	33.9618	34.1894	35.0011	36.1032	37.4666

Fig. 6 demonstrates the effect of rotational speed on first four natural frequencies of rotating FG tapered beam. It is also concluded that increasing the rotational speed leads to increase in higher mode frequencies. It is also interesting to note that the ascending pattern is more sensitive for the lower natural frequencies. For instance for FG beam with power-law exponent defined as  $n = 10$ , increasing normal rotational speed from 0 to 10, leads to about 207%, 53%, 21% and 12% increase in the first four natural frequencies respectively.

Finally, to demonstrate the effect of hub radius parameter on the non-dimensional frequencies of the FG rotating tapered beam, the variation of the first four natural frequencies with various hub

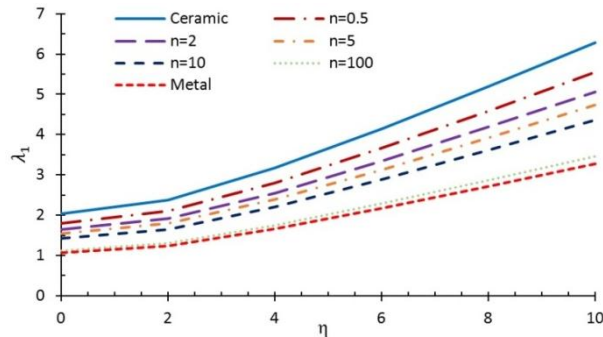


Fig. 5 The effect of rotational speed and power-law exponent on first non-dimensional natural frequency of FG rotating tapered beam ( $\delta = 0, n = 0.5, L/h = 10, \alpha = \beta = 0.1$ )

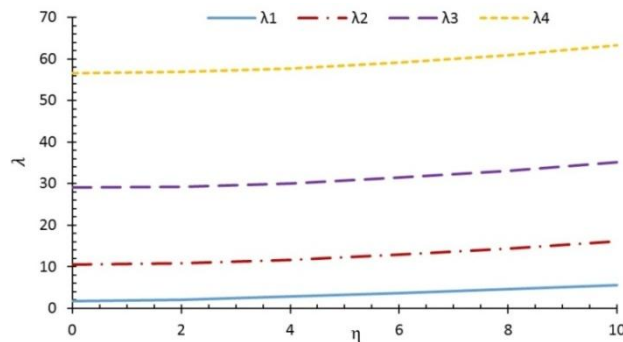


Fig. 6 The effect of rotational speed on first four non-dimensional natural frequencies of FG rotating tapered beam ( $\delta = 0, n = 0.5, L/h = 10, \alpha = \beta = 0.1$ )

Table 8 The effect of hub radius parameter on first four non-dimensional natural frequencies of FG rotating tapered beam ( $n = 5, L/h = 10, \alpha = \beta = 0.1$ )

$\eta$		$\delta$					
		0	0.2	0.4	0.6	0.8	1.0
2	$\lambda_1$	1.7911	1.8522	1.9113	1.9687	2.0243	2.0785
	$\lambda_2$	9.2585	9.3212	9.3835	9.4453	9.5068	9.5678
	$\lambda_3$	25.0087	25.0741	25.1392	25.2041	25.2689	25.3334
	$\lambda_4$	48.5410	48.6097	48.6783	48.7468	48.8152	48.8834
4	$\lambda_1$	2.3882	2.5661	2.7321	2.8840	3.0364	3.1773
	$\lambda_2$	9.9407	10.1720	10.3978	10.6185	10.8345	11.0460
	$\lambda_3$	25.7012	25.9536	26.2031	26.4499	26.6940	26.9356
	$\lambda_4$	49.2579	49.5275	49.7954	50.0615	50.3260	50.5888
6	$\lambda_1$	3.1262	3.4255	3.7001	3.9552	4.1943	4.4201
	$\lambda_2$	10.9837	11.4485	11.8940	12.3221	12.7348	13.1336
	$\lambda_3$	26.8121	27.3503	27.8764	28.3911	28.8949	29.3886
	$\lambda_4$	50.4274	51.0156	51.5958	52.1683	52.7332	53.2909

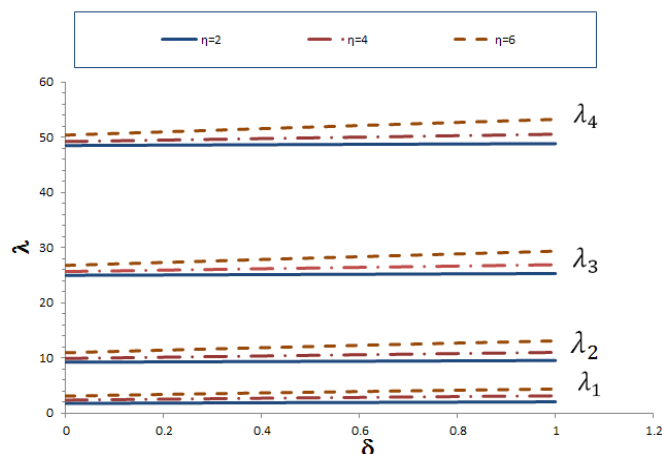


Fig. 7 Effect of hub radius parameter on first four non-dimensional natural frequencies of FG rotating tapered beam ( $n = 0.5$ ,  $L/h = 10$ ,  $\alpha = \beta = 0.1$ )

radius parameters is tabulated in Table 8. For a better insight and also in order to establish the trend, these effects are shown in Fig. 7 where the first four natural frequencies are plotted for three different values of the rotational speed parameter and for several values of the hub radius parameter.

It is observed that all frequencies increase with the hub radius as expected due to increase in centrifugal stiffening of the beam. Also the rate of increase becomes larger with the increasing rotational speed parameter because the centrifugal force is directly proportional to both of these parameters. For instance for FG beam with rotational speed parameter defined as  $\eta = 2$ , increasing the hub radius parameter from 0 to 1, leads to about 16% increase in the fundamental frequency while in the case of rotational speed parameter defined as  $\eta = 6$  this increase in hub radius parameter leads to about 41% increase in the fundamental frequency.

## 5. Conclusions

In this paper, free transverse vibration analysis of a rotating double tapered functionally graded beam is investigated within the framework of a semi-analytical technique called the differential transform method. Several important aspects such as taper ratios, hub radius and the rotational speed as well as the material volume fraction index which have impacts on natural frequencies of such beams are investigated and discussed in detail. The calculated results are compared with the ones in literature and great agreement is observed. The numerical results indicate that the flexural natural frequencies increase with rotational speed and hub radius while they decrease with the power-law exponent and this trend is almost the same for higher mode frequencies. It is also concluded that the fundamental frequency of tapered FG beams increase as the breadth and the height taper ratio increase while the higher mode frequencies increase with the breadth taper ratio and they decrease with the height taper ratio.

## References

Abdel-Halim Hassan, I.H. (2002), "On solving some eigenvalue problems by using a differential

- transformation”, *Appl. Math. Comput.*, **127**(1), 1-22.
- Alshorbagy, A.E., Eltahir, M.A. and Mahmoud, F.F. (2011), “Free vibration characteristics of a functionally graded beam by finite element method”, *Appl. Math. Model.*, **35**(1), 412-425.
- Attarnejad, R. and Shahba, A. (2011), “Basic displacement functions for centrifugally stiffened tapered beams”, *Int. J. Numer. Method. Biomed. Eng.*, **27**(9), 1385-1397.
- Attarnejad, R., Semnani, S.H. and Shahba, A. (2010), “Basic displacement functions for free vibration analysis of non-prismatic Timoshenko beams”, *Finite Elem. Anal. Des.*, **46**(10), 916-929.
- Balkaya, M., Kaya, M.O. and Sağlam, A. (2009), “Analysis of the vibration of an elastic beam supported on elastic soil using the differential transform method”, *Arch. Appl. Mech.*, **79**(2), 135-146.
- Belabed, Z., Houari, M.S.A., Tounsi, A., Mahmoud, S.R. and Anwar Bég, O. (2014), “An efficient and simple higher order shear and normal deformation theory for functionally graded material (FGM) plates”, *Compos.: Part B*, **60**, 274-283.
- Benatta, M.A., Mehab, I., Tounsi, A. and Adda Bedia, E.A. (2008), “Static analysis of functionally graded short beams including warping and shear deformation effects”, *Comput. Mater. Sci.*, **44**(2), 765-773.
- Bessaim, A., Houari, M.S.A., Tounsi, A., Mahmoud, S.R. and Adda Bedia, E.A. (2013), “A new higher-order shear and normal deformation theory for the static and free vibration analysis of sandwich plates with functionally graded isotropic face sheets”, *J. Sandw. Struct. Mater.*, **15**(6), 671-703.
- Bouderba, B., Houari, M.S.A. and Tounsi, A. (2013), “Thermomechanical bending response of FGM thick plates resting on Winkler–Pasternak elastic foundations”, *Steel Compos. Struct., Int. J.*, **14**(1), 85-104.
- Bouiadjra, R.B., Bedia, E.A. and Tounsi, A. (2013), “Nonlinear thermal buckling behavior of functionally graded plates using an efficient sinusoidal shear deformation theory”, *Struct. Eng. Mech., Int. J.*, **48**(4), 547-567.
- Bourada, M., Tounsi, A., Houari, M.S.A. and Adda Bedia, E.A. (2012), “A new four-variable refined plate theory for thermal buckling analysis of functionally graded sandwich plates”, *J. Sandw. Struct. Mater.*, **14**(1), 5-33.
- Bouremana, M., Houari, M.S.A., Tounsi, A., Kaci, A. and Adda Bedia, E.A. (2013), “A new first shear deformation beam theory based on neutral surface position for functionally graded beams”, *Steel Compos. Struct., Int. J.*, **15**(5), 467-479.
- Draiche, K., Tounsi, A. and Khalfi, Y. (2014), “A trigonometric four variable plate theory for free vibration of rectangular composite plates with patch mass”, *Steel Compos. Struct., Int. J.*, **17**(1), 69-81.
- Ebrahimi, F. (2013), “Analytical investigation on vibrations and dynamic response of functionally graded plate integrated with piezoelectric layers in thermal environment”, *Mech. Adv. Mater. Struct.*, **20**(10), 854-870.
- Ebrahimi, F., Rastgoo, A. and Atai, A.A. (2009a), “A theoretical analysis of smart moderately thick shear deformable annular functionally graded plate”, *Eur. J. Mech.-A/Solids*, **28**(5), 962-973.
- Ebrahimi, F. and Rastgoo, A. (2009b), “FSDPT based study for vibration analysis of piezoelectric coupled annular FGM plate”, *J. Mech. Sci. Technol.*, **23**(8), 2157-2168.
- Fazelzadeh, S.A. and Hosseini, M. (2007), “Aerothermoelastic behavior of supersonic rotating thin-walled beams made of functionally graded materials”, *J. Fluid. Struct.*, **23**(8), 1251-1264.
- Fazelzadeh, S.A., Malekzadeh, P., Zahedinejad, P. and Hosseini, M. (2007), “Vibration analysis of functionally graded thin-walled rotating blades under high temperature supersonic flow using the differential quadrature method”, *J. Sound Vib.*, **306**(1), 333-348.
- Hebali, H., Tounsi, A., Houari, M.S.A., Bessaim, A. and Adda Bedia, E.A. (2014), “New quasi-3D hyperbolic shear deformation theory for the static and free vibration analysis of functionally graded plates”, *J. Eng. Mech. (ASCE)*, **140**(2), 374-383.
- Houari, M.S.A., Tounsi, A. and Anwar Bég, O. (2013), “Thermoelastic bending analysis of functionally graded sandwich plates using a new higher order shear and normal deformation theory”, *Int. J. Mech. Sci.*, **76**, 102-111.
- Hodges, D.Y. and Rutkowski, M.Y. (1981), “Free-vibration analysis of rotating beams by a variable-order finite-element method”, *AIAA J.*, **19**(11), 1459-1466.
- Huang, Y. and Li, X.F. (2010), “A new approach for free vibration of axially functionally graded beams

- with non-uniform cross-section”, *J. Sound Vib.*, **329**(11), 2291-2303.
- Larbi, L.O., Kaci, A., Houari, M.S.A. and Tounsi, A. (2013), “An efficient shear deformation beam theory based on neutral surface position for bending and free vibration of functionally graded beams”, *Mech. Based Des. Struct. Mach.*, **41**(4), 421-433.
- Li, X.F. (2008), “A unified approach for analyzing static and dynamic behaviors of functionally graded Timoshenko and Euler–Bernoulli beams”, *J. Sound Vib.*, **318**(4), 1210-1229.
- Li, L., Zhang, D.G. and Zhu, W.D. (2014), “Free vibration analysis of a rotating hub–functionally graded material beam system with the dynamic stiffening effect”, *J. Sound Vib.*, **333**(5), 1526-1541.
- Mahi, A., Adda Bedia, E.A., Tounsi, A. and Mechab, I. (2010), “An analytical method for temperature-dependent free vibration analysis of functionally graded beams with general boundary conditions”, *Compos. Struct.*, **92**(8), 1877-1887.
- Meziane, M.A.A., Abdelaziz, H.H. and Tounsi, A. (2014), “An efficient and simple refined theory for buckling and free vibration of exponentially graded sandwich plates under various boundary conditions”, *J. Sandw. Struct. Mater.*, **16**(3), 293-318.
- Mohanty, S.C., Dash, R.R. and Rout, T. (2013), “Free vibration of a functionally graded rotating Timoshenko beam using FEM”, *Adv. Struct. Eng.*, **16**(2), 405-418.
- Nachum, S. and Altus, E. (2007), “Natural frequencies and mode shapes of deterministic and stochastic non-homogeneous rods and beams”, *J. Sound Vib.*, **302**(4), 903-924.
- Özdemir, Ö. and Kaya, M.O. (2006), “Flapwise bending vibration analysis of a rotating tapered cantilever Bernoulli–Euler beam by differential transform method”, *J. Sound Vib.*, **289**(1), 413-420.
- Piovan, M.T. and Sampaio, R. (2009), “A study on the dynamics of rotating beams with functionally graded properties”, *J. Sound Vib.*, **327**(1), 134-143.
- Pradhan, K.K. and Chakraverty, S. (2014), “Effects of different shear deformation theories on free vibration of functionally graded beams”, *Int. J. Mech. Sci.*, **82**, 149-160.
- Rajasekaran, S. (2013), “Free vibration of centrifugally stiffened axially functionally graded tapered Timoshenko beams using differential transformation and quadrature methods”, *Appl. Math. Model.*, **37**(6), 4440-4463.
- Saidi, H., Houari, M.S.A., Tounsi, A. and Adda Bedia, E.A. (2013), “Thermo-mechanical bending response with stretching effect of functionally graded sandwich plates using a novel shear deformation theory”, *Steel Compos. Struct., Int. J.*, **15**(2), 221-245.
- Shahba, A. and Rajasekaran, S. (2012), “Free vibration and stability of tapered Euler–Bernoulli beams made of axially functionally graded materials”, *Appl. Math. Model.*, **36**(7), 3094-3111.
- Şimşek, M. (2010), “Fundamental frequency analysis of functionally graded beams by using different higher-order beam theories”, *Nucl. Eng. Des.*, **240**(4), 697-705.
- Sina, S.A., Navazi, H.M. and Haddadpour, H. (2009), “An analytical method for free vibration analysis of functionally graded beams”, *Mater. Des.*, **30**(3), 741-747.
- Singh, K.V., Li, G. and Pang, S.S. (2006), “Free vibration and physical parameter identification of non-uniform composite beams”, *Compos. Struct.*, **74**(1), 37-50.
- Tounsi, A., Houari, M.S.A., Benyoucef, S. and Adda Bedia, E.A. (2013), “A refined trigonometric shear deformation theory for thermoelastic bending of functionally graded sandwich plates”, *Aerosp. Sci. Technol.*, **24**(1), 209-220.
- Zarrinzadeh, H., Attarnejad, R. and Shahba, A. (2012), “Free vibration of rotating axially functionally graded tapered beams”, *Proceedings of the Institution of Mechanical Engineers, Part G: Journal of Aerospace Engineering*, **226**, 363-379.
- Zhou, J.K. (1986), “Differential transformation and its applications for electrical circuits”, *Peoples Republic of China, Huazhong University Press, Wuhan, China*, pp. 1279-1289. [In Chinese]
- Zidi, M., Tounsi, A., Houari, M.S.A., Adda Bedia, E.A. and Anwar Bég, O. (2014), “Bending analysis of FGM plates under hygro-thermo-mechanical loading using a four variable refined plate theory”, *Aerosp. Sci. Technol.*, **34**, 24-34.